

Overcoming Interfacial Interactions with Electric Fields

T. Thurn-Albrecht, J. DeRouchey, and T. P. Russell*

Polymer Science and Engineering Department, University of Massachusetts, Amherst, Massachusetts 01003

H. M. Jaeger

James Franck Institute and Department of Physics, University of Chicago, Chicago, Illinois 60037

Received November 9, 1999; Revised Manuscript Received February 25, 2000

ABSTRACT: Electric fields have been shown to orient nanoscopic domains laterally in thin copolymer films effectively. To achieve an orientation normal to the surface, interfacial interactions impose a barrier. Using asymmetric diblock copolymers of polystyrene (PS) and poly(methyl methacrylate) (PMMA) having cylindrical microdomains, a threshold electric field strength E_t was found above which complete orientation of the cylindrical domains was achieved. This threshold field strength was independent of film thickness (for films $\sim 10\text{--}30\ \mu\text{m}$ thick) and could be described by the difference in interfacial energies of the components. At field strengths slightly below E_t a coexistence of the domains parallel and perpendicular to the electrode surface was found which is consistent with the introduction of defects via undulations in the structure as one proceeds away from the surface.

Introduction

Block copolymers offer a wealth of self-assembling, ordered, nanoscopic morphologies that have tremendous potential as lithographic templates, high-density porous media, or scaffolds for nanoscopic devices. Realizing the full potential of these materials in bulk or thin film applications, however, mandates control over the spatial orientation of the structures. External fields can be used to this end. These may be passive, as with interfacial interactions, or active, as with mechanical shear. In liquid crystal displays, for example, electric fields are used to control molecular alignment and, hence, the optical properties of the device. Much less attention has been devoted to amorphous systems where the anisotropies on the molecular level are small. Block copolymers are an exception where mechanical shearing¹ and electric fields^{2–4} have been used to produce well-ordered arrays of nanoscopic domains. However, in thin copolymer films, the orientation of the structures normal to the surface introduces an interesting twist. In particular, there is a competition between the applied electric field and interfacial interactions^{5–8} that gives rise to a threshold field strength that must be exceeded to fully align the morphology. This threshold field strength has revealed a novel means of determining differences in the interfacial energies of the components comprising the copolymer.

Theory

Electric Field Effects. When a dielectric body with a dielectric constant ϵ is placed in an electric field \vec{E}_0 , the polarization difference between the body and the surroundings will induce charges on the surface of the body. These surface charges give rise to a depolarization field \vec{E}_p superposed on the external field. Since, for an anisotropic body, the surface charges and, therefore, \vec{E}_p depend on the orientation of the body, the resulting electric field energy is also orientation dependent. Taking the state with no dielectric body present as a reference state, the free energy can be written as⁹

$$F = F_0 + F_{el} = F_0 - \frac{1}{2} \int_V \vec{E}_0 \cdot \vec{P} dV \quad (1)$$

F_{el} is the orientation dependent electrical contribution to the free energy, whereas F_0 contains all the contributions to the free energy independent of orientation. \vec{P} is the polarization inside the dielectric body having a volume V . The polarization is proportional to the total electric field $\vec{E}_0 + \vec{E}_p$,

$$\vec{P} = \chi \vec{E} = \chi (\vec{E}_0 + \vec{E}_p) \quad (2)$$

where χ is the polarizability, a constant for an isotropic material. To evaluate eq 1, the electric field \vec{E} has to be known, which generally requires solving Maxwell equations for the geometry under consideration. For the simple case of an infinitely long cylinder with its axis either parallel or perpendicular to the external field \vec{E}_0 , this solution can easily be constructed from the boundary conditions for the electric field at the interface.⁹ The state with the lowest free energy will be one of these two orientations, since only in these cases is the torque $\vec{K} = \vec{P} \times \vec{E}_0 = 0$. The resulting difference in the free energy between the two states with different orientations is

$$\Delta F = F_{\parallel} - F_{\perp} = \frac{1}{2} \vec{E}_0^2 \epsilon_0 (\epsilon - 1) \frac{1 - \epsilon}{1 + \epsilon} V \quad (3)$$

where ϵ_0 is the permittivity in a vacuum. If the surrounding medium has a dielectric constant ϵ_{ext} , ϵ has to be replaced by ϵ/ϵ_{ext} and ϵ_0 by $\epsilon_0\epsilon_{ext}$. Since ΔF is always negative, the orientation of the cylinder axis parallel to the applied field is the lower free energy state, whether $\epsilon > \epsilon_{ext}$ or $\epsilon < \epsilon_{ext}$. Amundson gave a similar solution for the more complex case of a regular array of cylinders assuming a weakly segregated structure.² Any effects of the electric field on the conformation of the polymers will not be considered here, since they are relevant only at electric field strengths much higher than that used in this study.¹⁰

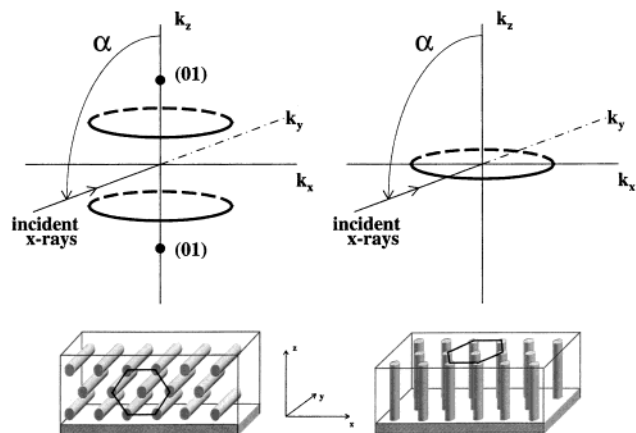


Figure 1. (A) Intensity distribution in reciprocal space for a hexagonal array of cylinders lying parallel to the surface of the film. A schematic of one grain of the cylinders is shown in the lower portion. In an actual sample, the grains are arranged randomly within the plane giving rise to the rings of diffraction parallel to the k_x - k_y plane. (B) The same as in (A), with the cylinders oriented normal to the surface. Again a schematic of one grain is shown. The incident X-ray angle, α , is changed by a rotation of the sample about the k_x axis. The diagrams shown correspond to $\alpha = 90^\circ$.

Experimental Section

Scattering from Oriented Hexagonally Close-Packed Cylinders. Shown in Figure 1a is a schematic diagram of reciprocal space for hexagonally packed cylinders having the (01) and (01) lattice planes parallel to the surface where there are many grains of this structure oriented randomly in the plane of the film. The rings result from a random orientation of grains in the plane of the film. By varying the angle of incidence α of the X-rays, defined with respect to the substrate normal ($\alpha = 0^\circ$), different points on the two rings of diffraction are observed. As α decreases from 90° to 0° , the scattering pattern changes from a six-point to a four-point and then to a two-point pattern at 30° . For $\alpha < 30^\circ$, the pattern disappears completely. The angle between the off-meridional reflections [(11), (11), (10), and (10)] and the meridian, $\Delta\Omega$, is related to α by

$$\Delta\Omega = \arcsin\left(\frac{1}{2}\sqrt{3 - \cot^2 \alpha}\right) \quad (4)$$

If the cylinders are oriented normal to the surface as in the rhs of Figure 1, the characteristic reflections appear in the k_x-k_y plane. Since there is no preferred orientation of grains of the hexagonal close-packed cylinders in the plane of the film, a ring of intensity is seen for $\alpha = 0$. For any other incidence angle, only two equatorial spots are evident.

Asymmetric diblock copolymers of polystyrene (PS) and poly(methyl methacrylate) P(S-*b*-MMA), having a weight-average molecular weight of 3.9×10^4 and polydispersity of 1.08 with a PMMA volume fraction of 0.29, were synthesized anionically. The order-to-disorder transition temperature of this copolymer was found to be $196 \pm 2^\circ\text{C}$ as determined by optical microscopy.^{11,12} Films of the copolymer were annealed between two $12.7\ \mu\text{m}$ Kapton sheets (separated by a Kapton spacer) that were coated on one side with 100 nm of Al which served as the electrodes. To avoid electric shorting, one of the Al electrodes was placed in direct contact with the polymer while the second was inverted with the Kapton in contact with the copolymer. Samples were heated into the disordered state under N_2 , and the voltage necessary to produce the desired electric field was applied. The sample was then cooled to 170°C into the ordered state and held at that temperature for 14 h. Subsequently, the sample was cooled to room temperature before the field was removed.

Ni-filtered Cu-K α radiation from a Rigaku rotating anode operated at 8 kW was used for small-angle X-ray scattering

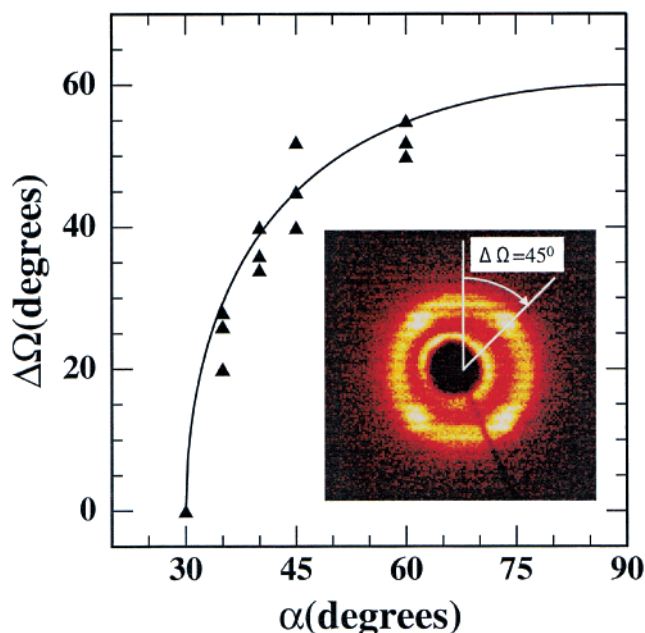


Figure 2. Azimuthal peak position $\Delta\Omega$ as a function of incidence angle α for an $86\ \mu\text{m}$ P(S-*b*-MMA) film annealed without an electric field. In the inset, the scattering observed at $\alpha = 45^\circ$ is shown.

(SAXS) measurements. The primary beam was collimated by a set of three pinholes. The sample was mounted on a rotation stage to change the angle of incidence α . A gas-filled area detector (Siemens Hi-Star) 1 m from the sample was used to record the scattering pattern. The flight path between the sample and the detector was evacuated. Typical exposure times for a $20\ \mu\text{m}$ sample were of the order of 30 min.

Results and Discussion

In the absence of an electric field, interfacial interactions force an alignment of the cylinders parallel to the substrate. This is demonstrated by the X-ray scattering pattern obtained from an $80\ \mu\text{m}$ film with $\alpha = 45^\circ$ shown in the inset of Figure 2. Consistent with the schematic diagram in Figure 1, four distinct reflections with a common $\Delta\Omega$ are seen at $q = 0.27\ \text{nm}^{-1}$ ($q = (4\pi/\lambda) \sin \theta$, λ is the X-ray wavelength, and 2θ is the scattering angle) corresponding to a lattice spacing of $L = 23.3\ \text{nm}$. As α changes, $\Delta\Omega$ at which the peaks are located changes. Plotted in Figure 2 is the dependence of $\Delta\Omega$ on α along with the solution to eq 4 (solid line). The agreement is quantitative, showing that the scattering arises from grains of hexagonally packed cylinders oriented parallel to the surface.

Samples of P(S-*b*-MMA) with thicknesses of 11, 20, and $30\ \mu\text{m}$ were annealed in an electric field up to field strengths of $25\ \text{V}/\mu\text{m}$. Morkved et al. showed that, in the absence of competing interfacial interactions, the cylindrical microdomains aligned parallel to the electric field lines at low field strengths, several $\text{V}/\mu\text{m}$.⁴ Here, however, an alignment of the cylinders parallel to the film surface, i.e., *normal* to the field lines, was maintained up to $11.5\ \text{V}/\mu\text{m}$. This difference is a direct consequence of the interfacial interactions of the copolymer with the electrode surfaces. Near $11.5\ \text{V}/\mu\text{m}$, as shown by the data in Figure 3a taken at $\alpha = 60^\circ$ for a $32\ \mu\text{m}$ sample, equatorial reflections are evident in addition to the four off-equatorial reflections. Consequently, there is a range in field strengths where both parallel and perpendicular alignment of the cylinders coexist. At higher field strength only two equatorial

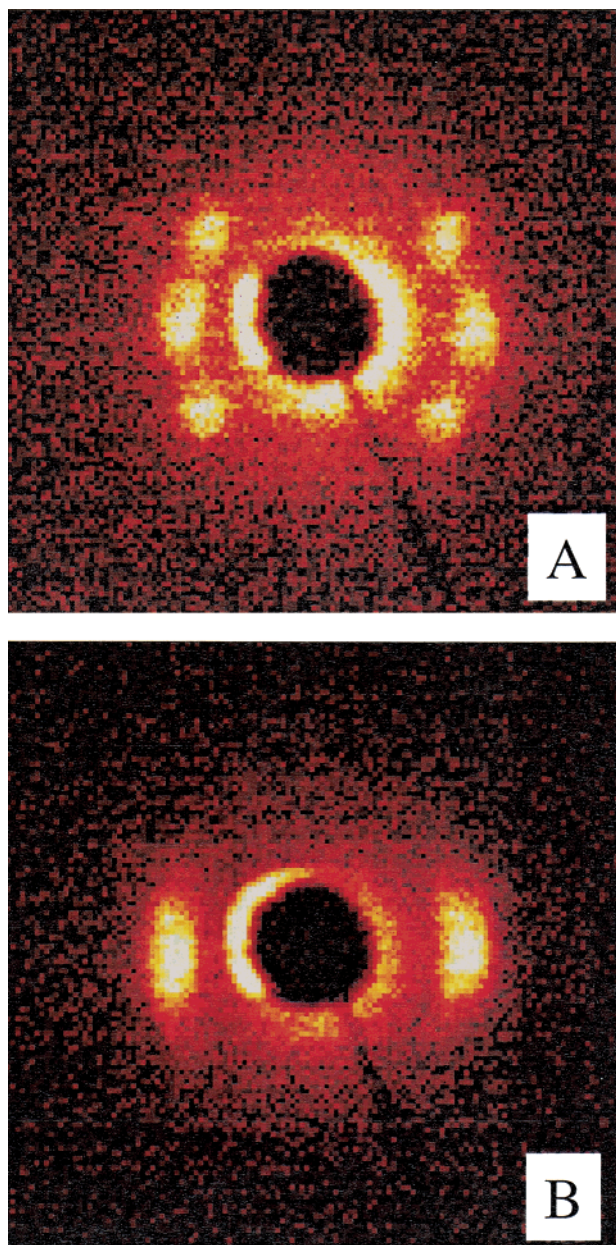


Figure 3. Scattering pattern measured at $\alpha = 60^\circ$ obtained from two samples annealed in an electric field. One sample (A) was annealed in an electric field of $9.9 \text{ V}/\mu\text{m}$ and the other (B) in a field of $14.5 \text{ V}/\mu\text{m}$. Scattering pattern (A) shows reflections indicative of cylinders oriented parallel, as well as perpendicular, to the substrate. In (B) only lateral reflections are seen indicative of cylinders oriented normal to the surface, i.e., parallel to the electric field lines.

reflections are seen as shown in Figure 3b for a $32 \mu\text{m}$ thick sample at $14.5 \text{ V}/\mu\text{m}$ with $\alpha = 60^\circ$. For high electric fields, the peak width generally approaches the resolution of the instrument. It should be noted that experiments on P(S-*b*-MMA) with a reverse composition, i.e., PS cylinders in a PMMA matrix, showed identical alignment behavior which is in keeping with eq 3.

The angle between the cylinder axis and the field lines is plotted as a function of field strength in Figure 4. In cases where both parallel and perpendicular alignment of the cylinders coexist, points were placed at 0° and 90° . As can be seen, there is a range in field strengths, from ~ 9.5 to $\sim 11.5 \text{ V}/\mu\text{m}$, where both orientations coexist. It should also be noted that the value obtained for the threshold field strength, $E_t = 11.5 \pm 1 \text{ V}/\mu\text{m}$, is

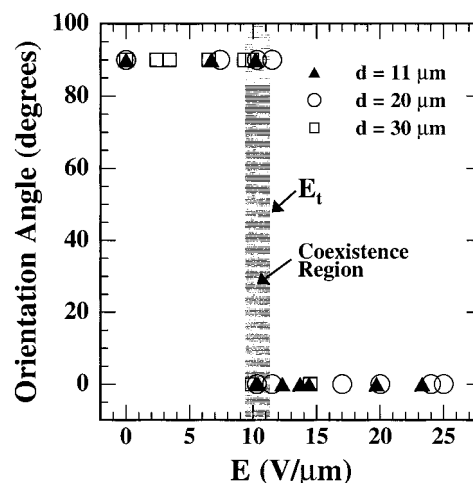


Figure 4. Orientation angle of the microstructure with respect to the field direction as a function of the electric field strength. A value of 90° corresponds to cylinders oriented parallel to the substrate, whereas 0° corresponds to cylinders oriented normal to the substrate, i.e., parallel to the field direction. The shaded region denotes a range in electric field strengths where both parallel and perpendicular cylinder alignment is observed. E_t is the threshold field strength, above which full alignment parallel to the applied field is observed.

independent of the thickness of the sample. These results clearly show that complete orientation of the cylindrical domains occurs only when $E > E_t$. For $E < E_t$ the orientation of a significant fraction of the cylinders is dictated by interfacial interactions.

The significance of E_t can be understood in terms of a simplified model for the free energy containing distinct contributions from interfacial interactions and electric field response. Modifying F in eq 1 to account for the surface contribution yields

$$F = F_0 + F_{\text{el}} + F_{\text{surf}} = F_0 - \frac{1}{2} \int_{V_{\text{el}}} \vec{E}_0 \cdot \vec{P}(\parallel, \perp) dV + \int_A \sigma(\parallel, \perp) dA \quad (5)$$

Here $\sigma(\parallel, \perp)$ is the contribution to the free energy over a surface area (A) due to interfacial interactions for parallel and perpendicular orientations of the cylinders, respectively. There is a competition between two forces, F_{surf} and F_{el} , which favor alignment of the cylinder axes perpendicular to and parallel to the electric field, respectively. V_{el} is the volume of the sample under the influence of the two competing forces. At the threshold field strength

$$\Delta F_{\text{el}} = -\Delta F_{\text{surf}} \quad (6)$$

Since E_t is independent of the film thickness, also, V_{el} does not vary with film thickness in keeping with the observed coexistence of both orientations near E_t . If the whole film contributed to the energy balance at $E = E_t$, it would follow from eq 6 that E_t scales as $1/\sqrt{d}$, since $F_{\text{el}} \propto E_0^2 d$. This is not the case, indicating that finite boundary layers adjacent to the electrode surfaces dominate F_{el} . The thickness of this surface layer is independent of the sample thickness. This implies that for thicker films the surface layer is less dominant since the defects necessary for coexistence of alignment parallel and perpendicular to the substrate can be accommodated more easily. Therefore, even at lower field strengths a large fraction of the sample is oriented by

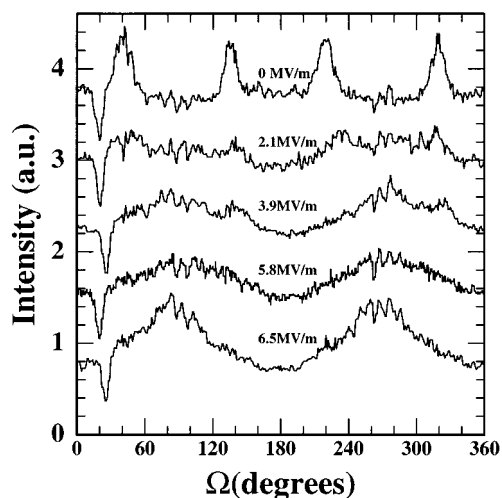


Figure 5. Azimuthal dependence of scattering intensity for a series of samples with a thickness of $86 \mu\text{m} \pm 10\%$ annealed at the different electric field strengths as indicated. The incidence angle is 45° , and the data have been offset for clarity.

the electric field, approaching bulk behavior.^{2,3} Measurements on an $86 \mu\text{m}$ thick sample annealed at electric fields well below E_t already show this behavior. The scattering intensity at $\alpha = 45^\circ$ and $q = 0.27 \text{ nm}^{-1}$ as a function of the azimuthal angle, Ω , for different field strengths is shown in Figure 5. Alignment of the morphology by the electric field can be observed at field strengths much less than E_t . For the sample annealed in the absence of an electric field, four peaks, indicative of alignment parallel to the sample surface, are seen. Even for field strengths as small as $2.1 \text{ V}/\mu\text{m}$, the intensity increases around $\Omega = 90^\circ$ and 270° , though the peaks characteristic of cylinders lying parallel to the surface are still visible. The widths of the reflections indicative of alignment normal to the substrate are larger than at higher electric field strengths, indicating that the degree of alignment increases with increasing electric field.

From eqs 3, 5, and 6 an estimate for ΔF_{el} at $E = E_t$ and, therefore, the difference in interfacial energies between the \parallel and \perp states can be calculated. If an upper limit of $10 \mu\text{m}$ for the thickness of the reorienting layer is assumed, the dielectric energy from eq 3, ΔF_{el} is $0.3 \times 10^{-3} \text{ J m}^{-2}$. Here, $\epsilon_0 = 8.854 \times 10^{-12} \text{ C}^2 \text{ J}^{-1} \text{ m}^{-1}$, $\epsilon_{PS} = 2.5$, $\epsilon_{PMMA} = 3.6$, and $E_t = 11.5 \text{ V}/\mu\text{m}$. With a volume fraction of the PMMA cylinders of 0.29, ΔF_{el} is calculated to be $\sim 1\%$ of the surface energies of PS or PMMA ($\sim 30 \times 10^{-3} \text{ J m}^{-2}$) and is approximately equal to the difference between the surface energies of these two polymers.¹³

The observation that the surface-induced orientation of the cylinders propagates into the interior of the film over distances large compared to the structural length scale of the copolymer is reminiscent of phenomena observed for liquid crystals. In terms of the elastic energy, a cylindrical block copolymer has the same symmetry as a columnar liquid crystal. In such a system it is not possible to change the orientation across a thin film from parallel to perpendicular to the surface without introducing defects. As long as the surface anchoring prevails, the response of the system to an electric field is not a reorientation of the structure but rather an undulation perpendicular to the axis of the cylinders.^{14,15} These Helfrich–Hurault undulations are

suppressed close to the interface but are amplified with increasing distance from the interface. A complete reorientation of the cylinders can only be realized when the applied field overcomes the interfacial interactions which occurs at E_t . Close to the threshold value of the electric field, in a situation where enough defects are present to build up a finite layer of cylinders aligned by the electric field, strong indications of structural rearrangement are observed even before complete orientation.

Conclusions

In conclusion, it has been shown that electric fields are an effective means of orienting copolymer domains normal to an interface. A thickness-independent field strength was found at which full alignment of the cylinders parallel to the field lines occurred. This threshold field strength is directly related to differences in the interfacial energies of the components. Slightly below this threshold field strength a coexistence of parallel and perpendicular alignment of the cylinders was found, resulting from the competition between the applied field and interfacial interactions. The studies presented here demonstrate the precise nature by which nanoscopic structures in thin films can be manipulated by the interplay of passive and active fields. The resulting structures, i.e., thin films containing arrays of nanoscopic cylinders oriented normal to the substrate, are promising candidates as templates for a variety of nanostructures.

Acknowledgment. We are grateful to C. Stafford for the synthesis of the sample material and to the Sheldahl Co. for supplying the aluminized Kapton. T. T.-A. acknowledges the support of the Deutsche Forschungsgemeinschaft. This work was also supported by the U.S. Department of Energy, Office Basic Energy Sciences, under Contract DE-FG02-96ER45612 and the National Science Foundation Materials Research Science and Engineering Center (DMR-9809365).

References and Notes

- (1) Hamley, I. W. *The Physics of Block Copolymers*; Oxford University Press: Oxford, 1998.
- (2) Amundson, K.; Helfand, E.; Quan, X.; Smith, S. D. *Macromolecules* **1993**, *26*, 2698.
- (3) Amundson, K.; Helfand, E.; Quan, X.; Hudson, S. D.; Smith, S. D. *Macromolecules* **1994**, *27*, 6559.
- (4) Morkved, T.; Lu, M.; Urbas, A. M.; Ehrichs, E. E.; Jaeger, H. M.; Mansky, P.; Russell, T. P. *Science* **1996**, *273*, 931.
- (5) Matsen, M. W. *Curr. Opin. Colloid Interface Sci.* **1998**, *3*, 1998.
- (6) Russell, T. P. *Curr. Opin. Colloid Interface Sci.* **1996**, *1*, 107.
- (7) Pickett, G. T.; Witten, T. A.; Nagel, S. R. *Macromolecules* **1993**, *26*, 3194.
- (8) Huang, E.; Russell, T. P.; Harrison, C.; Chaikin, P. M.; Register, R. A.; Hawker, C. J.; Mays, J. *Macromolecules* **1998**, *31*, 7641.
- (9) Landau, L. D.; Lifschitz, E. M. *Elektrodynamik der Kontinua*; Pergamon Press: Oxford, 1984.
- (10) Gurovich, E. *Phys. Rev. Lett.* **1995**, *74*, 482.
- (11) Balsara, N. P.; Perahia, D.; Safinya, C. R.; Tirrell, M.; Lodge, T. P. *Macromolecules* **1992**, *25*, 3896.
- (12) Amundson, K.; Helfand, E.; Patel, S. S.; Quan, Z.; Smith, S. D. *Macromolecules* **1992**, *25*, 1935.
- (13) Mansky, P.; Liu, Y.; Huang, E.; Russell, T. P.; Hawker, C. *Science* **1997**, *275*, 1458.
- (14) De Gennes, P. G.; Prost, J. *The Physics of Liquid Crystals*; Oxford University Press: Oxford, 1993.
- (15) Onuki, A.; Fukuda, J. *Macromolecules* **1995**, *28*, 8788.

MA991896Z